Journal of Alloys and Compounds 504 (2010) 508–513

Contents lists available at ScienceDirect

Journal of Alloys and Compounds

journal homepage: www.elsevier.com/locate/jallcom

Magnetic and ferroelectric properties of $PbFe_{1/2}Nb_{1/2}O_3$ synthesized by a solution precipitation method

D. Bochenek

University of Silesia, Department of Materials Science, 2, Śnieżna St., Sosnowiec 41-200, Poland

ARTICLE INFO

Article history:
Received 28 January 2010
Received in revised form 28 May 2010
Accepted 31 May 2010
Available online 11 June 2010

Keywords:
Multiferroics
Smart materials
Ferroelectromagnetics
Solution precipitation method
PFN ceramics

ABSTRACT

Results of an influence of the technological conditions on ferroelectric and magnetic properties of the $PbFe_{1/2}Nb_{1/2}O_3$ ceramics (PFN) are presented. Synthesizing of the PFN material was made by a chemical solution precipitation method and sintering (compacting) by a free sintering method. Temperatures of dehydratization, burning of an organic phase and crystallization of an amorphous powder were determined by the thermal analysis (TA) method.

The structure of PFN ceramics examined by X-ray diffraction was found to be perovskite-like. Microstructural examinations, the electric conductivity and tests of the ferroelectric and magnetic properties were performed. The magnetic susceptibility measurements have shown that the samples show an antiferromagnetic transition at high temperature (T_{N1}) and it is followed by an antiferromagnetic like transition at low temperature (T_{N2}). It has been shown that in the technological process used the optimum compacting conditions are revealed by the ceramics sintered at 1050 °C for 2 h.

1. Introduction

The ferroic is a general term covering ferromagnetics (FM), ferroelectrics (FE), ferroelastics (FES) and ferrotoroidies. Materials showing at least two out of four possible ordered states are called multiferroics [1,2]. Biferroic $PbFe_{1/2}Nb_{1/2}O_3$ (PFN) belongs to a group of the multiferroics, in which there is simultaneous ordering of an electric subsystem (at $T < T_{CE} \approx 114$ °C) and a magnetic subsystem (at $T < T_N \approx -130$ °C) in the specified temperature ranges [3,4]. PFN has a structure of the perovskite type with general formula $A(B'B'')O_3$, where ions of iron and niobium substitute for octahedral B′ and B″ positions at random, whereas lead is placed in positions A.

A mutual influence of the magnetic and electric subsystem in ferroelectromagnetics causes that the PFN ceramics becomes an interesting material for a production of multifunctional intelligent elements, namely those which react strongly to different types of external stimuli [5,6].

Microelectrical engineering developing at a great speed imposes higher and higher requirements for properties of the functional ceramics produced for different elements and electronic components [7–10]. The extreme values of parameters and their time and temperature stability depend on both a chemical composition of the ceramics and a production process. The optimum values of the electric, magnetic, mechanical and thermal parameters and their time stability depend, among others, on chemical homogeneity and the ceramic microstructure.

In the case of the ferroelectromagnetic PFN ceramics there are a lot of special powder synthesizing techniques such as a molten salt synthesis, a reaction sintering, columbite, sol–gel, co-precipitation method and others [11,12]. Each of these methods has both disadvantages and advantages but they require an application of specific technological conditions and accuracy of the process performance.

The sol–gel method and its numerous variations are the methods which enable to obtain a powder of the optimum parameters. Use of those methods in the PFN synthesizing technology ensures to obtain high purity of the products and enables to conduct the synthesis at a significantly lower temperature and it results in a decrease in evaporation of the components and facilitates preservation of the stoichiometric composition.

A chemical solution precipitation method is one of the variations of the sol–gel method. It provides for convenient and effective conditions of the ceramic powder synthesizing. It is based on the reactions in solutions of precursors—organic or inorganic metal salts of high purity. Organic metal salts (acetates, alcoholates) or inorganic compounds (e.g. nitrates, metal hydroxides) can be the initial materials to prepare the chemical solution.

Looking for the optimum PFN synthesis method and a technology of the solution precipitation, using the ferric citrate as the main precursor, is presented in this work. An influence of the sintering temperature on basic properties of the PFN ceramics has been examined as well.

2. Experimental details

The $PbFe_{1/2}Nb_{1/2}O_3$ ceramics was obtained as a result of the chemical method of the solution precipitation using the following precursors: ferric citrate monohydrate $C_6H_5FeO_7 \cdot H_2O$ (Fluka) pure p.a., lead (II) acetate trihydrate

E-mail addresses: dariusz.bochenek@us.edu.pl, dbochene@us.edu.pl.

0925-8388/$ – see front matter © 2010 Elsevier B.V. All rights reserved.
doi:10.1016/j.jallcom.2010.05.153

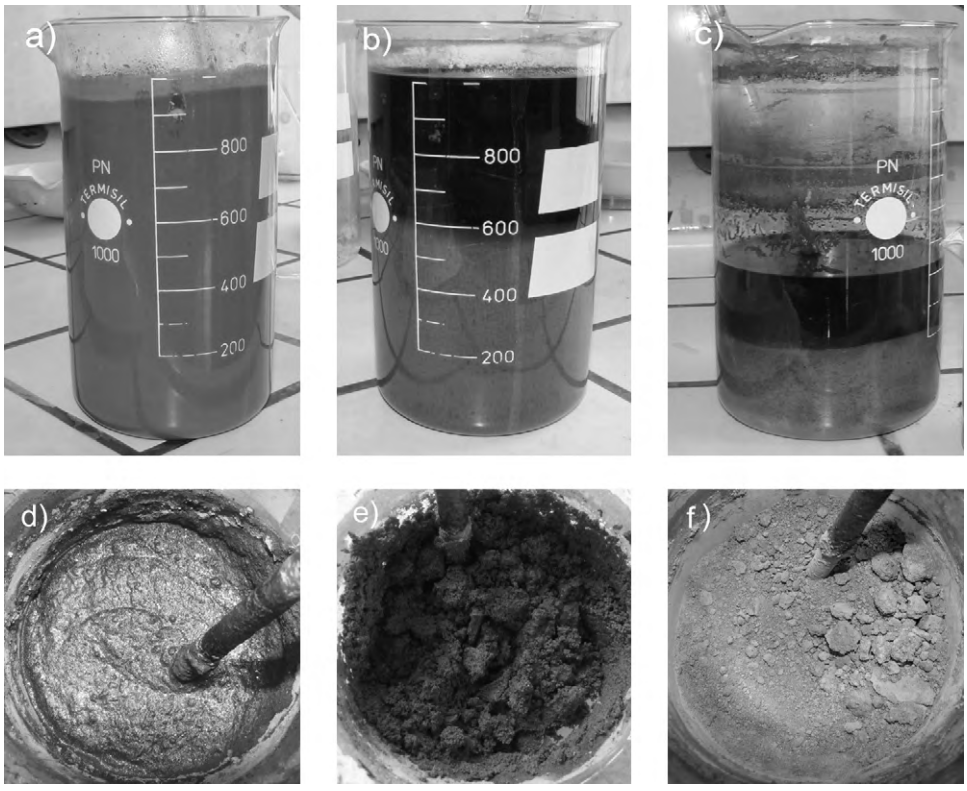

Fig. 1. The PFN ceramics powder obtained by the solution precipitation method: (a) the solution with beginning of the precipitation, (b and c) the precipitation process, (d and e) the solvent vaporization as a result of the IR lamp effect on the solution, (f) the PFN powder formed.

(ACS) $Pb(CH_3COO)_2{\cdot}3H_2O$ (POCh) pure p.a. and niobium (V) ethoxide $Nb(OC_2H_5)_5$ (Aldrich) 99.95%. The solution precipitation method is a variation of the PFN sol–gel synthesizing.

$Pb(CH_3COO)_2{\cdot}3H_2O$ weighed out with allowance was dissolved in the CH_3COOH acetic acid. Then, $Nb(OC_2H_5)_5$ was weighed out and ethylene glycol with 2-methoxyethanol was added. The distilled water was added to the third component in the PFN technology (that is ferric citrate $C_6H_5FeO_7{\cdot}H_2O$), and then the solution was heated. The acetic acid (80%) was added to the solution to increase effectiveness of dissolving and it was brought to boiling while stirring intensively. All the component solutions prepared in the above way were mixed, heated in the heating jacket. After mixing the substance changes into a turbid solution, in which the precipitation process takes place. After adding the acetylacetone the solution is orange-red. The distilled water was added for the hydrolysis to take place, and the process proceeded rapidly. The solution was dried under an IR lamp in order to vaporize the solvent and to obtain PFN in a form of a powder.

The synthesis process of the $PbFe_{1/2}Nb_{1/2}O_3$ material carried out by the solution precipitation method is presented in Fig. 1.

The powder was stirred after complete drying, and then it was subjected to baking (calcination) to remove organic parts. A calcination temperature of the PFN material organic parts was selected on basis of a thermal analysis (DTA and TG) on a Q-1500D derivatograph (with Paulik–Paulik–Erdey system) in the temperature range of 20–1000 °C. Two exothermal peaks (at the temperatures about 280 °C and about 370 °C) are observed on the DTA curves before the calcination of the organic parts (Fig. 2a). These peaks are connected with evaporation of the water residues and a decomposition of the organic parts, which is accompanied by the TG mass loss (4.11%). No further peaks and the mass loss are observed in the DTA and TG curves above 410 °C. After the calcination process of the organic parts (Fig. 2b) no peaks originating from the changes taking place in the material are found.

The following conditions of calcination to remove organic parts on basis of thermal analysis were qualified: the calcination temperature T_{w1} = 600 °C, the calcination time t_w = 3 h.

After removal of the organic part the PFN powder was stirred, and then it was pressed into compacts (in the steel matrix by the cold uniaxial pressing ~100 MPa) and they were free sintered (FS) in the Al_2O_3 bed for 2 h at temperatures T_s = 1000 °C (PFN1), 1050 °C (PFN2) and 1100 °C (PFN3). Free sintering was conducted in the electric chamber furnace of a Termod KS-1350 type, where atmospheric pressure was the sintering medium. An adjustable temperature control ensured its linear increase and good stability (a furnace temperature measurement error was ±0.3%).

The X-ray examinations were made on a polycrystalline diffractometer of the Phillips firm with a Cu lamp and a graphite monochromator. The microstructure examinations were made by a SEM scanning microscope HITACHI S-4700 with EDS Noran Vantage system, dielectric measurements were performed on a capacity bridge of a QuadTech 1920 Precision LCR Meter type, with a heating rate of 0.5°/min, at different frequency of the measurement field (from 100 Hz to 20 kHz) and the hysteresis loop with use of a high voltage feeder of a Matsusada Precision

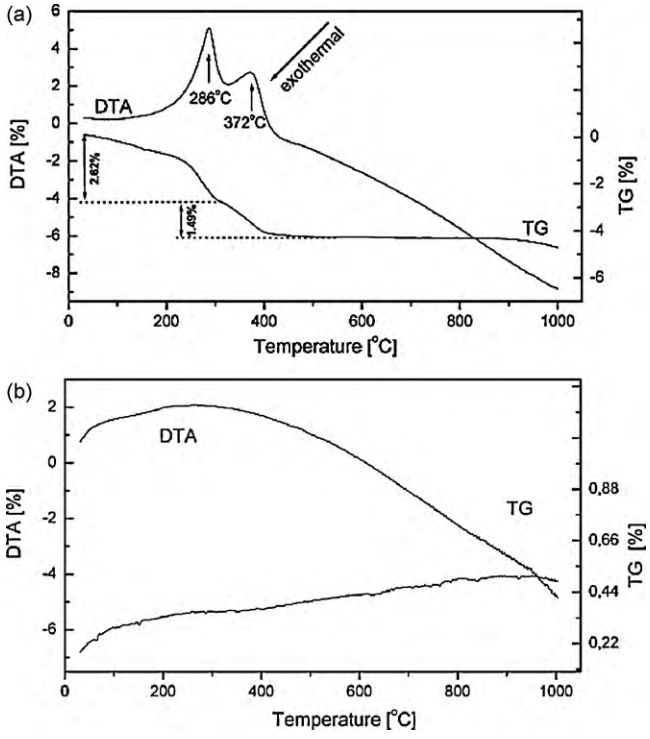

Fig. 2. DTA and TG of a PFN powders (a) before and (b) after removal of organic parts.

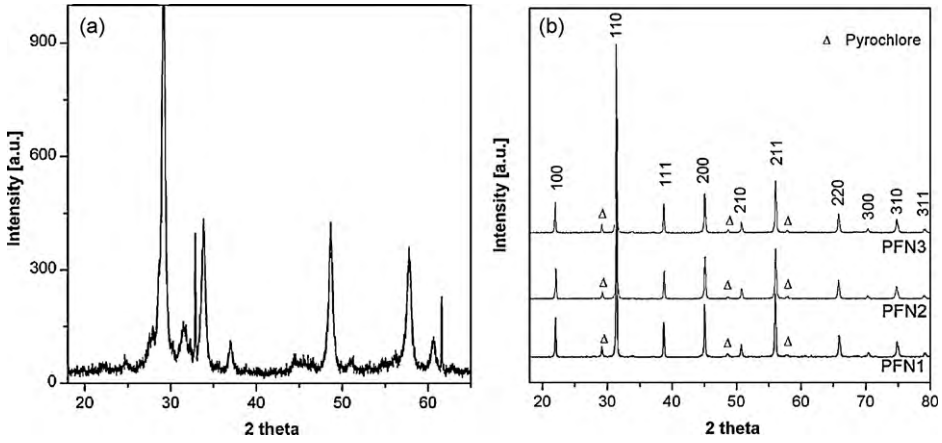

Fig. 3. X-ray diffraction pattern for the PFN powders (a) after removing of organic parts and (b) after sintering at temperatures 1000 °C (PFN1), 1050 °C (PFN2), 1100 °C (PFN3).

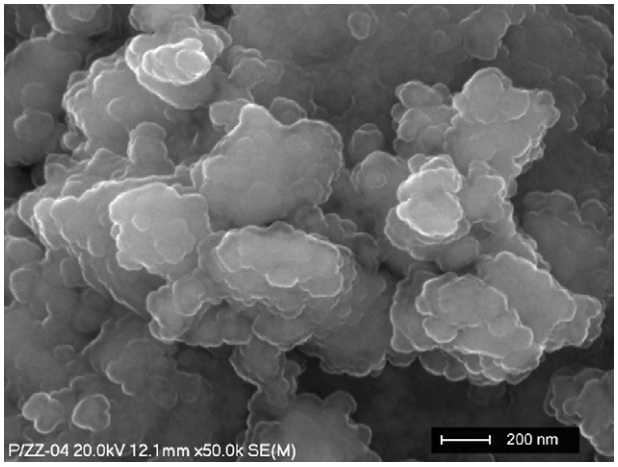

Fig. 4. The SEM images of the PFN powder used to obtain the PFN ceramics.

Inc. HEOPS-5B6 type. The DC measurements were carried out with the use of the Cahn magnetic balance in the temperature range of −270 °C to 75 °C.

The percentage content of the P_f perovskite phase was calculated from the following relationship:

$$P_f = \frac{I_{1\,10}\,100}{I_{110} + I_{222}}[\%]. \quad (1)$$

where I_{110} and I_{222} are intensities of the (1 1 0) perovskite and (2 2 2) pyrochlore diffraction lines.

3. Results and discussion

The X-ray diffraction of the PFN material powders after removal of the organic part is presented in Fig. 3a. The X-ray diffractions for the PFN ceramics (for different sintering temperatures) are presented in Fig. 3b. It can be observed that a perovskite structure of the PFN material is formed completely after the sintering process (ceramic compacting). At room temperature this material is characterized by a tetragonal structure with a small amount of a pyrochlore phase. For PFN1 P_f = 95.02%, for PFN2 P_f = 96.20%

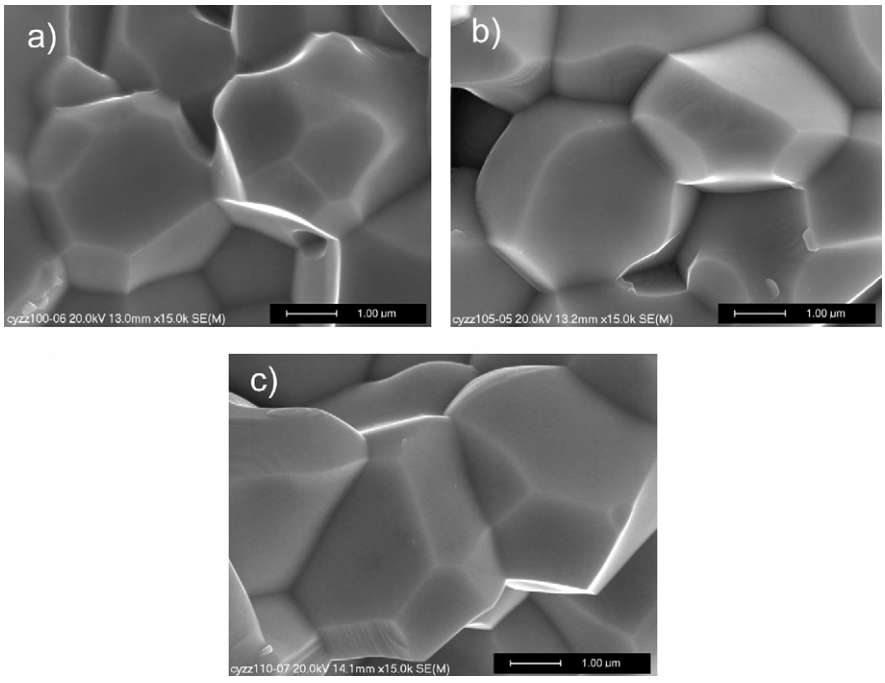

Fig. 5. An influence of the sintering temperature on the microstructure of the PFN ceramics sintered at the temperature of (a) 1000 °C (PFN1), (b) 1050 °C (PFN2), (c) 1100 °C (PFN3).

Table 1
The $PbFe_{1/2}Nb_{1/2}O_3$ ceramics parameters obtained by the solution precipitation method.

$PbFe_{1/2}Nb_{1/2}O_3$	PFN1	PFN2	PFN3
Temperature sintering	1000 °C	1050 °C	1100 °C
ρ_{exp} (g/cm^3)	7.47	7.60	7.31
$\rho_{exp}/\rho_{theor} \times 100$ (%)	88.3	89.9	86.4
ρ_{DC} at T_r (Ω m)	8.85×10^7	7.24×10^8	1.64×10^7
a (Å)	4.0207	4.0231	4.0228
c (Å)	4.0145	4.0205	4.0102
V (Å)	64.90	65.07	64.90
ρ_{DC} at T_m (Ω m)	1.02×10^7	4.50×10^7	1.16×10^6
E_a at I (eV)	0.35	0.33	0.40
E_a at II (eV)	0.72	0.92	0.14
E_a at III (eV)	0.94	0.80	1.09
T_m (°C)	90	91.5	92.8
ε_r	1690.00	1650	1850
$(\tan\ \delta)_{T_r}$	0.047	0.040	0.080
ε_m	5110	5600	7240
$(\tan\ \delta)_{T_m}$	0.137	0.083	0.122
$\varepsilon_m/\varepsilon_r$	3.02	3.40	3.91
α	1.64	1.62	1.69

Theoretical density (ρ_{theor}) value of PFN is ~8.457 g/cm^3.

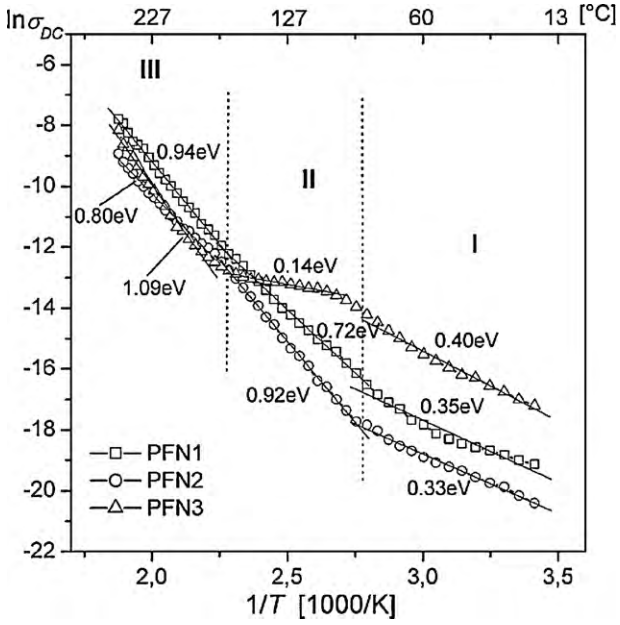

Fig. 6. An influence of the sintering temperature on the $\ln \sigma_{DC}(1/T)$ temperature relationships for the PFN ceramics.

whereas for PFN3 P_f = 94.88%. The specimen sintered at 1050 °C contains the lowest amount of the foreign non-perovskite pyrochlore phase.

SEM images of the PFN material powder from which the ceramic specimens have been obtained are presented in Fig. 4. The PFN powder consists of fine elements joined into bigger agglomerates. The optimum sintering conditions are shown by specimen PFN2 (the sintering temperature 1050 °C and time 2 h), what is exhibited by a correctly formed grain of the microstructure visible in the SEM images of the specimen fracture (Fig. 5b). This PFN ceramic sample shows the largest apparent density (Table 1). The sintering temperature of 1000 °C and the sintering time of 2 h do not provide for good conditions for grain formation (Fig. 5a), whereas higher sintering temperature 1100 °C causes excessive grain growth (Fig. 5c).

The PFN ceramics obtained by the conventional methods has high electric conductivity (low values of resistivity) [13,14]. In the case of the solution precipitation technology resistivity values are within a range from 1.64×10^7 Ω m to 7.24×10^8 Ω m. The PFN2 ceramics sintered at 1050 °C shows the highest values of the direct current resistivity at room temperature and at the Curie temperature (Table 1). The temperature courses of the direct current conductivity logarithm of the PFN specimens $-\ln \sigma_{DC}(1/T)$ in the area of the phase transition show characteristic changes (Fig. 6), what is manifested by a change of the E_a activation energy value (I in the ferroelectric phase and II in the paraelectric phase). A subsequent change of the activation energy value is observed in the paraelectric phase (III) at a higher temperature.

The PFN ceramics obtained by the solution precipitation method has relatively favourable dielectric parameters (Table 1). The temperature courses of electric permittivity are presented in Fig. 7. An increase in the sintering temperature of the PFN ceramics does not move a phase transition temperature significantly. It causes, however, an increase in the maximum value of the electric permittivity. A decrease in the diffusion of the phase transition is also observed.

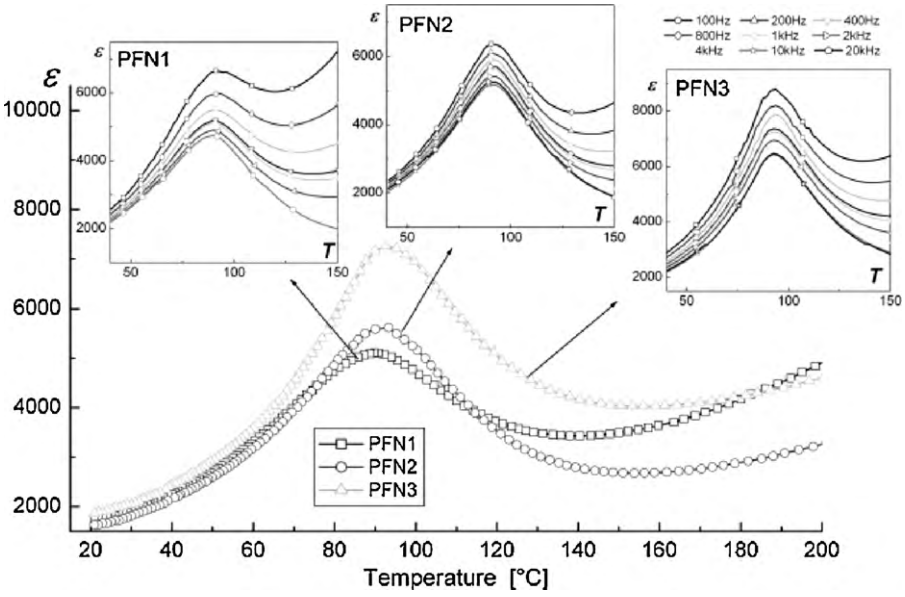

Fig. 7. An influence of the sintering temperature on temperature dependences of electric permittivity ε on temperature T for the PFN ceramics obtained by the solution precipitation method (ν = 1 kHz). Inside the $\varepsilon(T)$ diagrams for the PFN ceramics at frequency ν = 100 Hz – 20 kHz (a cooling cycle).

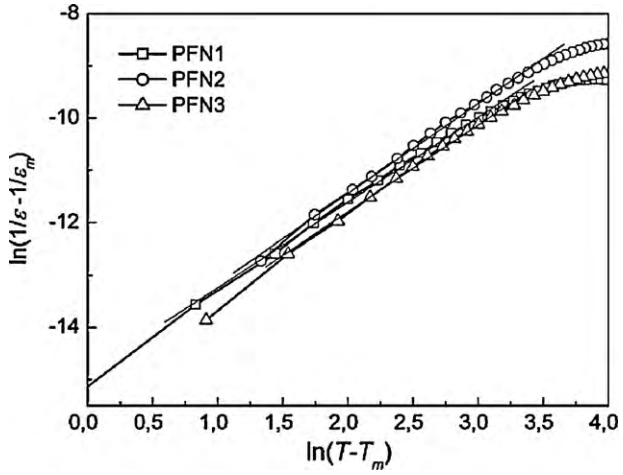

Fig. 8. The plots of $\ln(1/\varepsilon - 1/\varepsilon_m)$ vs. $\ln(T - T_m)$ for the PFN ceramics at temperatures higher than T_m.

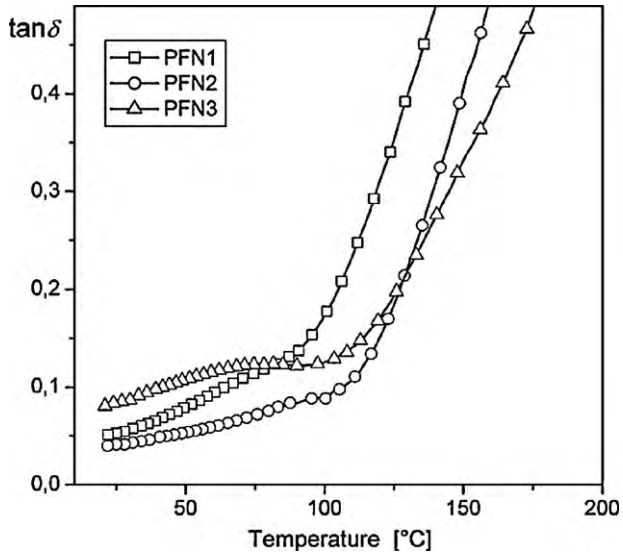

Fig. 9. An influence of the sintering temperature on the temperature dependences of the dielectric loss angle tangent $\tan\delta$ on temperature T for the PFN ceramics obtained by the solution precipitation method ($\nu = 1$ kHz).

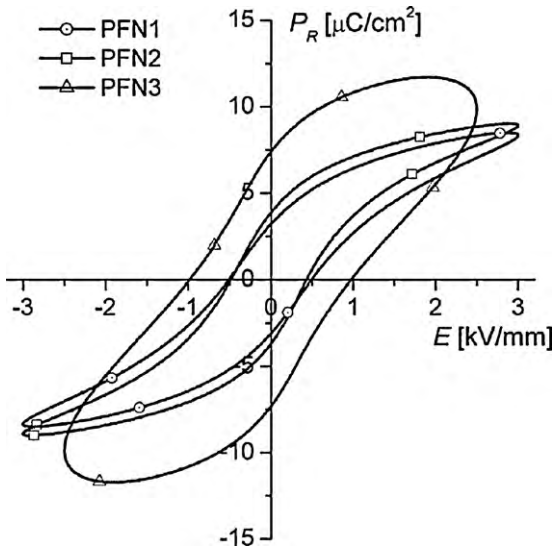

Fig. 10. Influence of the temperature sintering on the hysteresis loops of the PFN ceramics.

The characteristic feature of the PFN material is lack of presence of a frequency displacement of the phase transition temperature, which is so characteristic for relaxors (the diagrams inside Fig. 7).

Plots of $\ln(1/\varepsilon - 1/\varepsilon_m)$ vs. $\ln(T - T_m)$ for PFN ceramics are illustrated in Fig. 8 and linear fitting was performed. The calculated values of the α parameter being a degree of the phase transition diffusion are presented in Table 1. The ceramic samples sintered at 1050 °C show the lowest degree of the diffusion from the group of the PFN ceramics.

The PFN ceramics obtained by the solution precipitation method, in which the ferric citrate ($C_5H_5FeO_7 \cdot H_2O$) was used as a basic precursor, shows relatively low dielectric losses (Fig. 9) comparing to the PFN ceramics obtained by other technologies e.g.: sintering of simple oxides in the solid phase [15], a one stage synthesizing method [16] or in a case of the PFN ceramics production by the sol–gel method with use of the ferric nitrate ($Fe(NO_3)_3 \cdot 3H_2O$) [17] or the ferric oxalate ($FeC_2O_4 \cdot 3H_2O$). The PFN ceramics sintered at 1050 °C for 2 h shows the lowest values of the dielectric losses both at room temperature and the phase transition temperature.

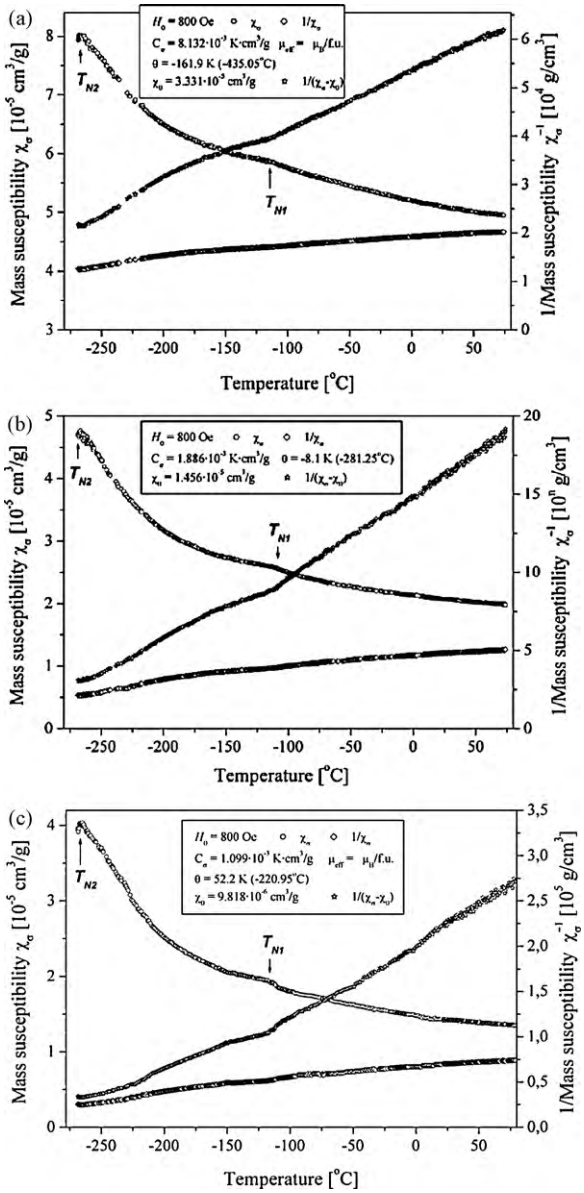

Fig. 11. Influence of the temperature sintering on the magnetic mass susceptibility (χ_σ) and inverse mass susceptibility ($1/\chi_\sigma$) of PFN (a) PFN1, (b) PFN2, (c) PFN3.

Electric hystersis loops of the PFN ceramics obtained at room temperature are presented in Fig. 10. The specimens sintered at lower temperatures (PFN1 and PFN2) show saturation of the hysteresis loop and similar values of the E_C coercion field (0.51 kV/mm and 0.46 kV/mm, respectively) and the P_r residual polarization (3.20 μC/cm^2 and 3.88 μC/cm^2, respectively).

Apart from the ferroelectric properties, the PFN ceramics has also magnetic properties. Temperature diagrams of magnetic susceptibility χ and an inverse of magnetic susceptibility $1/\chi$ for the PFN ceramics are presented in Fig. 11. A small peak (T_{N1}) below −110 °C and a second peak more visible (T_{N2}), at temperature about −265 °C are observed on the $\chi(T)$ courses. The anomalies observed in the diagrams are connected with occurrence of phase transitions in the magnetic material. Similar results of magnetic examinations are presented in work [18], where the magnetic measurements showed an antiferromagnetic transition at temperatures T_{N1} due to the superexchange interactions mediated by Fe–O–Fe and an additional antiferromagnetic type transition at T_{N2}.

It is observed (Fig. 11) that values of magnetic susceptibility decrease with an increase in the PFN ceramics sintering temperature, but the character of curves $\chi(T)$ does not change.

4. Conclusions

The $PbFe_{1/2}Nb_{1/2}O_3$ material obtained by the solution precipitation method shows an advantageous set of dielectric, magnetic and ferroelectric parameters. This kind of the ceramics has relatively low electric conductivity besides low dielectric losses and high values of electric permittivity. The magnetic measurements show that the PFN ceramic samples undergo two antiferromagnetic transitions: at a high temperature (T_{N1}) and at a low temperature (T_{N2}).

The performed technological tests of an influence of the technological process on the dielectric properties and electric conductivity of the PFN ceramics have shown that the optimum sintering temperature is 1050 °C during 2 h. The specimens obtained in those technological conditions show the optimum parameters in the PFN ceramics group analyzed.

Occurrence of both magnetic and ferroelectric properties in the PFN material (biferroics) widens application possibilities comparing to materials of ferroic properties.

Acknowledgement

This article was realized within the framework of research project NR15000504.

References

[1] B.B. Van-Aken, J.P. Rivera, H. Schmid, M. Fiebig, Nature 449 (2007) 702–705.
[2] K.F. Wang, J.M. Liu, Z.F. Ren, Adv. Phys. 58 (2009) 321–448.
[3] D. Bochenek, Z. Surowiak, Phys. Status Solidi A 206 (2009) 2857–2865.
[4] W. Peng, N. Lemée, J. Holc, M. Kosec, R. Blinc, M.G. Karkut, J. Magn. Magn. Mater. 321 (2009) 1754–1757.
[5] R. Blinc, P. Cevc, A. Zorko, J. Holc, M. Kosec, Z. Trontelj, J. Pirnat, N. Dalal, V. Ramachandran, J. Krzystek, J. Appl. Phys. 101 (2007) 033901.
[6] M.H. Lente, J.D.S. Guerra, G.K.S. de Souza, B.M. Fraygola, C.F.V. Raigoza, D. Garcia, J.A. Eiras, Phys. Rev. B 78 (2008) 054109.
[7] J. Tang, M. Zhu, T. Zhong, Y. Hou, H. Wang, H. Yan, Mater. Chem. Phys. 101 (2007) 475–479.
[8] B.-J. Fang, C.-L. Ding, W. Liu, L.-Q. Li, L. Yang, Eur. Phys. J. Appl. Phys. 45 (2009) 20302.
[9] P. Yang, S. Peng, X.B. Wu, J.G. Wan, X.M. Lu, F. Yan, J.S. Zhu, J. Phys. D: Appl. Phys. 42 (2009) 015005.
[10] S. Sahoo, R.N.P. Choudhary, B.K. Mathur, Phys. Status Solidi B 246 (2009) 1377–1381.
[11] C. Bharti, A. Dutta, S. Shannigrahi, S.N. Choudhary, R.K. Thapa, T.P. Sinha, J. Electron. Spectrosc. Relat. Phenom. 169 (2009) 80–85.
[12] R. Sun, W. Tan, B. Fang, Phys. Status Solidi A 206 (2009) 326–331.
[13] O. Raymond, R. Font, N. Suarez, J. Portelles, J.M. Siqueiros, J. Appl. Phys. 97 (2005) 084107.
[14] L.N. Korotkov, S.N. Kozhukhar', V.V. Posmet'ev, D.V. Urazov, D.F. Rogovoi, Yu.V. Barmin, S.P. Kubrin, S.I. Raevskaya, I.P. Raevskii, Tech. Phys. 54 (2009) 1147–1155.
[15] D. Bochenek, Eur. Phys. J. Spec. Top. 154 (2008) 15–18.
[16] D. Bochenek, J. Dudek, Eur. Phys. J. Spec. Top. 154 (2008) 19–22.
[17] D. Bochenek, Z. Surowiak, J. Alloys Compd. 480 (2009) 732–736.
[18] V.V. Bhat, K.V. Ramanujachary, S.E. Lofland, A.M. Umarji, J. Magn. Magn. Mater. 280 (2004) 221–226.